0026-895X/05/6804-1049–1060$20.00
MOLECULAR PHARMACOLOGY
Vol. 68, No. 4
13888/3051879
Mol Pharmacol 68:1049–1060, 2005
Printed in U.S.A.

N-Methyl-*N′*-nitro-*N*-nitrosoguanidine Activates Cell-Cycle Arrest through Distinct Mechanisms Activated in a Dose-Dependent Manner

Dillon I. Beardsley, Wan-Ju Kim, and Kevin D. Brown

Department of Biochemistry and Molecular Biology and the UF Shands Cancer Center, University of Florida College of Medicine, Gainesville, Florida

Received April 18, 2005; accepted June 30, 2005

ABSTRACT

S_N1-alkylating agents, such as the mutagenic and cytotoxic drug *N*-methyl-*N′*-nitro-*N*-nitrosoguanidine (MNNG), robustly activate the DNA damage-responsive G_2 checkpoint. Establishment of this checkpoint is dependent on a functional mismatch repair (MMR) system; however, exposure to high doses of MNNG overrides the requirement for MMR to trigger G_2 arrest. In addition, unlike moderate-dose exposure, in which the G_2 checkpoint is attenuated in ataxia-telangiectasia, mutated (ATM)-deficient cells, high-dose MNNG treatment activates G_2 arrest through an ATM-independent mechanism. We document that this arrest is sensitive to the pharmacological agents caffeine and 7-hydroxystaurosporine (UCN-01) that inhibit the checkpoint kinases ATM/ATM and Rad-3–related (ATR) and Chk1/Chk2, respectively. Furthermore, these agents block inactivation of the cell-cycle regulatory molecules Cdc25C and Cdc2, establishing the downstream mechanism through which high-dose MNNG establishes G_2 arrest. Activation of both Chk2 and Chk1 was independent of ATM and MMR in response to high-dose MNNG, unlike the response to moderate doses of this drug. Chk2 was found to be dispensable for cell-cycle arrest in response to high-dose MNNG treatment; however, ATR deficiency and decreased Chk1 expression forced by RNA interference resulted in diminished checkpoint response. These results indicate that MNNG activates the G_2 checkpoint through different mechanisms activated in a dose-dependent fashion.

N-Methyl-*N′*-nitro-*N*-nitrosoguanidine (MNNG) is a nitrosourea and a monofunctional S_N1-alkylating agent. MNNG and related genotoxic agents are extremely mutagenic, carcinogenic, and evoke a strong cell-cycle arrest and/or apoptotic response. MNNG methylates various nucleophilic centers within the DNA molecule, with methylation of the N^3 position of adenine and the N^7 and O^6 positions of guanine being the predominant lesions. N^3MeA and N^7MeG lesions are efficiently repaired by base excision repair (BER). However, the cytotoxic and mutagenic properties of MNNG are believed to principally stem from the methylation of the O^6 position of guanine (Karran and Bignami, 1992; Stojic et al., 2004a). Direct repair of mutagenic O^6MeG lesions is accomplished by the repair protein methylguanine-DNA methyltransferase (MGMT). Therefore, lost or diminished MGMT activity results in MNNG-induced increased lesion load and sensitivity to MNNG (Kalamegham et al., 1988).

In addition to direct repair, O^6MeG lesions are recognized by the mismatch repair (MMR) system (Griffin et al., 1994; Duckett et al., 1996). MMR is an evolutionarily conserved DNA repair mechanism that is chiefly responsible for resolving postreplicative mismatches in DNA (Modrich and Lahue, 1996). Furthermore, MMR has been proposed to play an active role during response to MNNG-induced DNA damage. In particular, exposure to MNNG and related methylators results in robust establishment of G_2 arrest, and MMR-deficient cells are unable to activate either cell-cycle arrest and/or apoptosis in response to these drugs (Goldmacher et al., 1986; Kat et al., 1993; Koi et al., 1994; Meikrantz et al., 1998). The inability of MMR-deficient cells to respond to MNNG-induced genotoxic insult has been termed alkylation tolerance (Branch et al., 1993; Kat et al., 1993).

The molecular basis of the alkylation-tolerant phenotype and the mechanistic involvement of the MMR system in growth arrest or apoptogenic signaling is the subject of much

This study was funded by grant R01-CA102289 from the National Institutes of Health (to K.D.B.).
Article, publication date, and citation information can be found at http://molpharm.aspetjournals.org.
doi:10.1124/mol.105.013888.

ABBREVIATIONS: MNNG, *N*-methyl-*N′*-nitro-*N*-nitrosoguanidine; MGMT, methylguanine-DNA methyltransferase; ATM, ataxia-telangiectasia, mutated; ATR, ataxia-telangiectasia, mutated, and Rad-3–related; IR, ionizing radiation; DSB, double-strand break; AP, apurinic/apyrimidinic; MMR, mismatch repair; RNAi, RNA interference; siRNA, short interfering RNA; BER, base excision repair; UCN-01, 7-hydroxystaurosporine; Ad-Cre, adenovirus-expressing Cre recombinase; ssDNA, single-stranded DNA; MMS, methyl-methane sulfonate; PBS, phosphate-buffered saline.

attention. Several groups observed that, in response to MNNG, MMR-deficient cells display defective ATR-dependent activation of the kinase Chk1 (Wang and Qin, 2003; Stojic et al., 2004b; Adamson et al., 2005). Our lab has determined recently, in response to a moderate MNNG dose, that MMR-deficient cells display both faulty Chk1 and Chk2 activation and that both of these kinases are required to fully activate G_2 arrest (Adamson et al., 2005).

The structurally unrelated Chk1 and Chk2 kinases both phosphorylate the cell-cycle regulatory Cdc25C phosphatase at the Ser216 residue in vitro (Sanchez et al., 1997; Ahn et al., 2000; Matsuoka et al., 2000). Phosphorylation of Cdc25C consequently targets this protein for interaction with 14-3-3 proteins that facilitate Cdc25C nuclear export (Peng et al., 1997; Lopez-Girona et al., 1999). Removal of Cdc25C from the nuclear compartment relieves inhibitory phosphorylation of the cyclin-dependent kinase Cdc2 (Strausfeld et al., 1991; Lee et al., 1992). Thus, Chk1/Chk2-induced Cdc25C inhibition forms a molecular basis for the G_2 checkpoint by inhibiting the activation of Cdc2 and restricting entry into mitosis.

Activation of Chk2 in response to γ-irradiation is dependent on direct phosphorylation by the ATM kinase (Ahn et al., 2000; Matsuoka et al., 2000). On the other hand, the ATM and Rad-3–related kinase ATR activates Chk1 in response to genotoxic insult (Liu et al., 2000; Zhao and Piwnica-Worms, 2001). Both ATR and Chk1 are required for activation of the G_2 checkpoint in response to IR and other genotoxins (Sanchez et al., 1997; Liu et al., 2000; Zhao and Piwnica-Worms, 2001). In contrast, cells deficient in ATM show no gross defects in the triggering of G_2 arrest in response to IR; rather, ATM-deficient cells are unable to arrest advance into mitosis immediately after γ-irradiation (Paules et al., 1995; Xu et al., 2002). Likewise, cells deficient in Chk2 are able to trigger the G_2/M checkpoint in response to IR (Jallepalli et al., 2003). These findings support the view that the ATR/Chk1 pathway is the dominant mechanism controlling the G_2 checkpoint in response to γ-irradiation. However, several recent reports have highlighted a role for Chk2 in triggering G_2 arrest in response to various stimuli (Masrouha et al., 2003; Castedo et al., 2004; Singh et al., 2004; Wei et al., 2005).

Our previous investigation focused on the molecular basis of MMR-dependent cell-cycle arrest in response to MNNG, and we documented that MMR-deficient cell lines treated with a high dose of this drug robustly activated the G_2 checkpoint. Other groups have also observed MMR-independent activation of this checkpoint in cells treated with high doses of MNNG (Jaiswal et al., 2004; Stojic et al., 2005). Herein, we report the mechanisms responsible for this high-dose response and contrast these results with the pathways controlling the response to moderate doses of this alkylating agent.

Materials and Methods

Cell Culture and Drug Treatment. The SV40-immortalized A-T fibroblast line AT22IJE-T stably expressing full-length recombinant human ATM (designated YZ-5) or stably transfected with empty vector (designated EBS-7) were cultured as indicated previously (Ziv et al., 1997). The MLH1-deficient human colorectal adenocarcinoma line HCT116 and its derivative (HCT116+ch3) were cultured with or without 400 μg/ml G418 as outlined previously (Koi et al., 1994; Umar et al., 1997). $ATR^{flox/-}$ cells (Cortez et al., 2001) were obtained from Dr. S. Elledge (Baylor College of Medicine, Houston, TX). To abrogate ATR expression in these cells, 1.0 μl (1×10^6 pfu/μl) of adenovirus-expressing Cre recombinase (Ad-Cre) was added to cultures for 2 days. HCT116 $Chk2^{-/-}$ (Jallepalli et al., 2003) were obtained from Drs. B. Vogelstein and F. Bunz (Johns Hopkins Cancer Center, Baltimore, MD). All cell lines were grown at 37°C in a humidified 5% CO_2 incubator. ATM, ATR, Chk2, or MLH1 expression was confirmed in appropriate mutant and control lines by immunoblotting.

MNNG treatment was performed by removing media from cultures of logarithmically growing cells and adding serum-free media. MNNG was then added to the indicated final concentration, and cells were returned to the incubator. After a 1-h drug exposure, the plates were rinsed extensively with PBS, and the cells were refed on complete growth media and returned to the incubator. MNNG (Aldrich Chemical Co., Milwaukee, WI) was dissolved in 0.1 M sodium acetate, pH 5.0, at a stock concentration of 10 mM and stored at −20°C. UCN-01 was obtained from the Developmental Therapeutics Program of the National Cancer Institute (National Institutes of Health, Bethesda, MD). A 10 mM stock solution of this drug was stored at −80°C. UCN-01 was added to cell cultures (500 nM final concentration) 45 min before MNNG treatment. Cells were maintained on UCN-01 both during and after MNNG exposure until cells were harvested and analyzed. Caffeine (Sigma Chemical, St. Louis, MO) was diluted in PBS at a stock concentration of 100 mM and stored at room temperature. Caffeine (5 mM final concentration) was added 1 h before MNNG treatment and was maintained in the medium during and after MNNG exposure.

Flow Cytometry. For quantitative analysis of cellular DNA content by flow cytometry, cells were harvested by trypsinization, washed with PBS, fixed in ice-cold 70% ethanol, and stored at −20°C for a minimum of 24 h. Before analysis, cells were washed twice in PBS followed by a 30-min room temperature incubation in PBS containing 25 μg/ml propidium iodide and 100 μg/ml RNase A. Cells were analyzed using a FACSCalibur flow cytometer (BD Biosciences, San Jose, CA), and >10,000 events were plotted using CellQuest software. Cell-cycle distribution was calculated using ModFit LT 3.0 software (Verity Software House, Topsham, ME).

Immunoblot Analysis. SDS-PAGE and immunoblotting procedures were conducted as outlined previously (Adamson et al., 2002). Membranes were probed with antibodies directed against total ATM (AM-9) (Allen et al., 2001), total Chk1 (Santa Cruz Biotechnology, Inc., Santa Cruz, CA), phospho-Ser317 Chk1 (Cell Signaling Technology Inc., Beverly, MA), total Chk2 (Santa Cruz Biotechnology), phospho-Thr68 Chk2 (Santa Cruz Biotechnology), total Cdc2 (Santa Cruz Biotechnology), phospho-Tyr15 Cdc2 (Cell Signaling), Cdc25C (Santa Cruz Biotechnology), SMC1 (Bethyl Laboratories, Montgomery, TX), or tubulin (a gift from Dr. D. W. Cleveland, University of California, San Diego, San Diego, CA), as indicated. Peroxidase-conjugated secondary antibodies were obtained from Kirkegaard and Perry Laboratories (Gaithersburg, MD) and immunoblot signals detected using Pico-West chemiluminescent substrate (Pierce Chemical, Rockford, IL). Immunoblot signals were quantified using NIH Image software (version 1.63).

Anti-ATR antiserum was created in our laboratory by isolating a ~1.1-kilobase segment of the human ATR mRNA transcript by reverse-transcriptase polymerase chain reaction (nucleotides 5294–6321 of the ATR ORF). Thereafter, this cDNA was subcloned as a BamHI/EcoRI fragment into the prokaryotic expression vector pGEX-4T, and clones were verified by automated sequencing. The encoded glutathione *S*-transferase-ATR fusion protein (ATR amino acids 1765–2107) was induced by the addition of 1 mM isopropyl β-D-thiogalactoside to a logarithmically growing culture of TOP-10 (Invitrogen, Carlsbad, CA) *Escherichia coli* harboring this plasmid. The fusion protein was found to be insoluble; thus, inclusion bodies were isolated. This material was used to immunize three adult New Zealand White rabbits, and one of these rabbits was found to display positive immunoreactivity by immunoblotting after initial immunization and two boosts at 3-week intervals. The resultant antiserum

(pAb-ATR39) was used routinely at a dilution of 1:5000 for immunoblot analysis. Rabbit immunization and housing was conducted by Open Biosystems (Huntsville, AL).

Cell Fractionation. Cells were separated into nuclear and cytoplasmic fractions using NE-PER Nuclear and Cytoplasmic Extraction Reagents as outlined by the manufacturer (Pierce). After lysing cells with supplied buffers, nuclei were harvested by centrifugation in a microcentrifuge (5 min, 16,000*g*, 4°C). Cytoplasmic (supernatant) and nuclear (pellet) fractions were separated and stored at −80°C before immunoblot analysis.

RNA Interference. Pooled synthetic siRNA duplexes (SMARTpool siRNA) specific for Chk1 and Nontargeting siRNA were purchased from Dharmacon (Lafayette, CO). For siRNA transfection, HCT116 Chk2$^{-/-}$ or HCT116+ch3 cells were seeded into six-well tissue culture plates at a density of 5×10^5 cells/well 24 h before transfection. Just before transfection, medium was removed, and 1 ml of complete growth medium (without antibiotics) was added to each well. Thereafter, 200 μl of reaction mix containing 5 μl of a 20 μM siRNA stock and 2 μl of Oligofectamine (Invitrogen) diluted in Opti-MEM was added to each well. After an overnight incubation at 37°C, the cells were split at a 1:4 ratio and then cultured overnight. The following day, the cells were transfected a second time as outlined above. Twenty-four hours after the second transfection, cells were washed, refed on complete growth medium, and treated with 5 or 25 μM MNNG for 1 h. MNNG-treated cells were cultured for 48 h and subsequently harvested and fixed for flow cytometry or lysates formed for immunoblot analysis.

Results

High-Dose MNNG Exposure Overrides ATM and MMR-Dependent G_2 Arrest Observed in Response to Moderate Drug Dose. A previous study from our laboratory that addressed the mechanisms responsible for activating the G_2 checkpoint in response to the S_N1-alkylating agent MNNG showed that this response was both ATM and MMR-dependent (Adamson et al., 2005). In particular, treatment of matched ATM-proficient/deficient and MMR-proficient/deficient cell lines with a moderate dose of MNNG (i.e., 5 μM) resulted in a blunted checkpoint response in ATM-deficient cells and a complete abrogation of arrest in MMR-deficient cells. However, we also observed that cells deficient in ATM and MMR display normal arrest in response to an increased dose of MNNG. To illustrate this point, we treated the isogenic ATM-proficient, YZ-5, and ATM-deficient EBS-7 lines with 5 μM MNNG and with 25 μM MNNG (high dose) and analyzed cells 48 h after drug treatment by flow cytometry. G_2 arrest was attenuated in the ATM-deficient EBS-7 cell line in response to 5 μM MNNG (Fig. 1A) compared with response in the isogenic ATM-proficient YZ-5 line (Fig. 1B). In contrast, robust G_2 arrest at this time point was observed after exposure to 25 μM MNNG in both YZ-5 and EBS-7 cells.

MNNG response was also examined using the MMR-deficient HCT116 and MMR-proficient HCT116+ch3 colorectal tumor cell lines in parallel experiments. MMR-deficient HCT116 cells were unable to activate the G_2 checkpoint 48 h after exposure to 5 μM MNNG treatment (Fig. 1C). In contrast, HCT116+ch3 cells displayed a robust G_2 arrest in response to 5 μM MNNG exposure (Fig. 1D). Both HCT116 and HCT116+ch3 cells treated with 25 μM MNNG displayed a substantial G_2 arrest 48 h after drug treatment (Fig. 1, C and D, respectively). Taken together, these results indicate that high-dose MNNG treatment activates the G_2 checkpoint through an ATM and MMR-independent mechanism(s). For clarity, we refer to moderate-dose MNNG exposure as the MNNG dose that activates a MMR-dependent G_2 arrest, whereas high-dose exposure is that dose which activates an MMR-independent checkpoint response.

We determined previously that checkpoint response to moderate doses of MNNG was ablated by the pharmacological agents caffeine and UCN-01. Caffeine is a potent inhibitor of the PIK-like protein kinase family (Sarkaria et al., 1998, 1999), and two of the members of this family (ATM and ATR) are linked to genotoxin-induced activation of G_2 arrest (Abraham, 2001). We pretreated EBS-7 and HCT116 cells with 5 mM caffeine before 25 μM MNNG exposure and maintained the cells on 5 mM caffeine until the cells were harvested 48 h after MNNG treatment and subsequently analyzed by flow cytometry. We observed that caffeine treatment resulted in nearly complete abrogation of G_2 arrest in both EBS-7 (Fig. 1E) and HCT116 (Fig. 1F) compared with cells treated with 25 μM MNNG in the absence of caffeine. Cells treated with caffeine alone showed no G_2 arrest consistent with this agent inhibiting damage-induced signaling.

UCN-01 (7-hydroxystaurosporine) is a strong inhibitor of the cell cycle kinase Chk1 (Graves et al., 2000) and the functionally related, yet structurally dissimilar, Chk2 kinase (Yu et al., 2002). Similar to caffeine treatment, EBS-7 and HCT116 cells were treated and maintained on 500 nM UCN-01 after exposure to 25 μM MNNG. We observed that UCN-01 abrogated G_2 arrest 48 h after 25 μM MNNG exposure in both EBS-7 and HCT116 lines (Fig. 1, E and F, respectively). Cells treated with UCN-01 only showed no apparent cell cycle arrest indicating that this drug is inhibiting signaling in response to MNNG. The results of these experiments using pharmacological inhibitors connect high-dose MNNG response and conserved ATM/ATR and Chk1/Chk2-dependent pathways.

High-Dose MNNG Exposure Activates G_2 Arrest Via Inhibition of the Cell-Cycle Regulatory Molecules Cdc25C and Cdc2. Previous work from our laboratory indicated that G_2 arrest in response to moderate doses of MNNG is attributable, at least in part, to inactivation of Cdc25C and Cdc2 (Adamson et al., 2005). Therefore, we next examined these downstream biochemical mechanisms during high-dose MNNG-induced response. In particular, we assessed nuclear retention of the cell-cycle phosphatase Cdc25C and accumulation of catalytically inactive cyclin-dependent kinase Cdc2 after exposure to 25 μM MNNG. Analysis of isolated EBS-7 nuclei harvested 48 h after 25 μM MNNG demonstrated a striking decrease in the nuclear levels of Cdc25C in these cells after high-dose MNNG exposure (Fig. 2A). As shown previously (Adamson et al., 2005), this ATM-deficient line does not dramatically down-regulate nuclear levels of Cdc25C in response to 5 μM MNNG. Although slight fluctuations in nuclear Cdc25C abundance were observed, these experiments clearly indicate that this molecule was maintained at a high level in cells treated with a combination of MNNG and caffeine or MNNG and UCN-01. These results indicate that these pharmacological inhibitors inhibit G_2 arrest through a blockade of Cdc25C export from the nucleus in response to high-dose MNNG. Parallel experiments were carried out on the MMR-deficient HCT116, and identical results were obtained (Fig. 2B). These findings indicate that exposure to high-dose MNNG leads to marked decreases in Cdc25C abundance within the nucleus of both ATM and

MMR-deficient cell lines at the time of optimal G_2 arrest similar to ATM and MMR-proficient cell lines treated with moderate doses of MNNG (Adamson et al., 2005).

Next, whole-cell lysates from MNNG-treated EBS-7 and HCT116 cells were immunoblotted with the phospho-Tyr15 Cdc2-specific antibody. Phosphorylation of Cdc2 at residue Tyr15 inhibits the catalytic activity of this cyclin-dependent kinase, and accumulation of Tyr15-phosphorylated Cdc2 is correlated with G_2 arrest (Kharbanda et al., 1994). In EBS-7 cells treated with 5 μM MNNG, we observed a modest accumulation of inactive Cdc2 (Fig. 2C). This result is consistent with the attenuated checkpoint response displayed by this line in response to a moderate dose of MNNG. In response to 25 μM MNNG, however, we observed a striking level of Tyr15-phosphorylated Cdc2 48 h after drug exposure. Accumulation of phosphorylated Cdc2 was blocked in cells pretreated and maintained on either caffeine or UCN-01 along with 25 μM MNNG exposure. These results indicate that these pharmacological inhibitors block G_2 arrest through a block of Cdc2 inactivation. Again, similar results were obtained in parallel experiments conducted on HCT116 cells (Fig. 2D). The only notable difference between MNNG response in HCT116 and EBS-7 cells is that HCT116 cells show no increase in Tyr15-phosphorylated Cdc2 in response to 5 μM MNNG exposure. This finding is consistent with the abrogated checkpoint activation shown by this MMR-deficient line after treatment with 5 μM MNNG. In summary, these findings indicate that, similar to response to a moderate MNNG dose, high-dose MNNG exposure activates G_2 arrest through inactivation of both Cdc25C and Cdc2.

Activation of Chk1 and Chk2 Do Not Require Either ATM or MMR in Response to High-Dose MNNG Treatment. We reported recently that in response to a moderate dose of MNNG, activation/phosphorylation of both Chk1 and

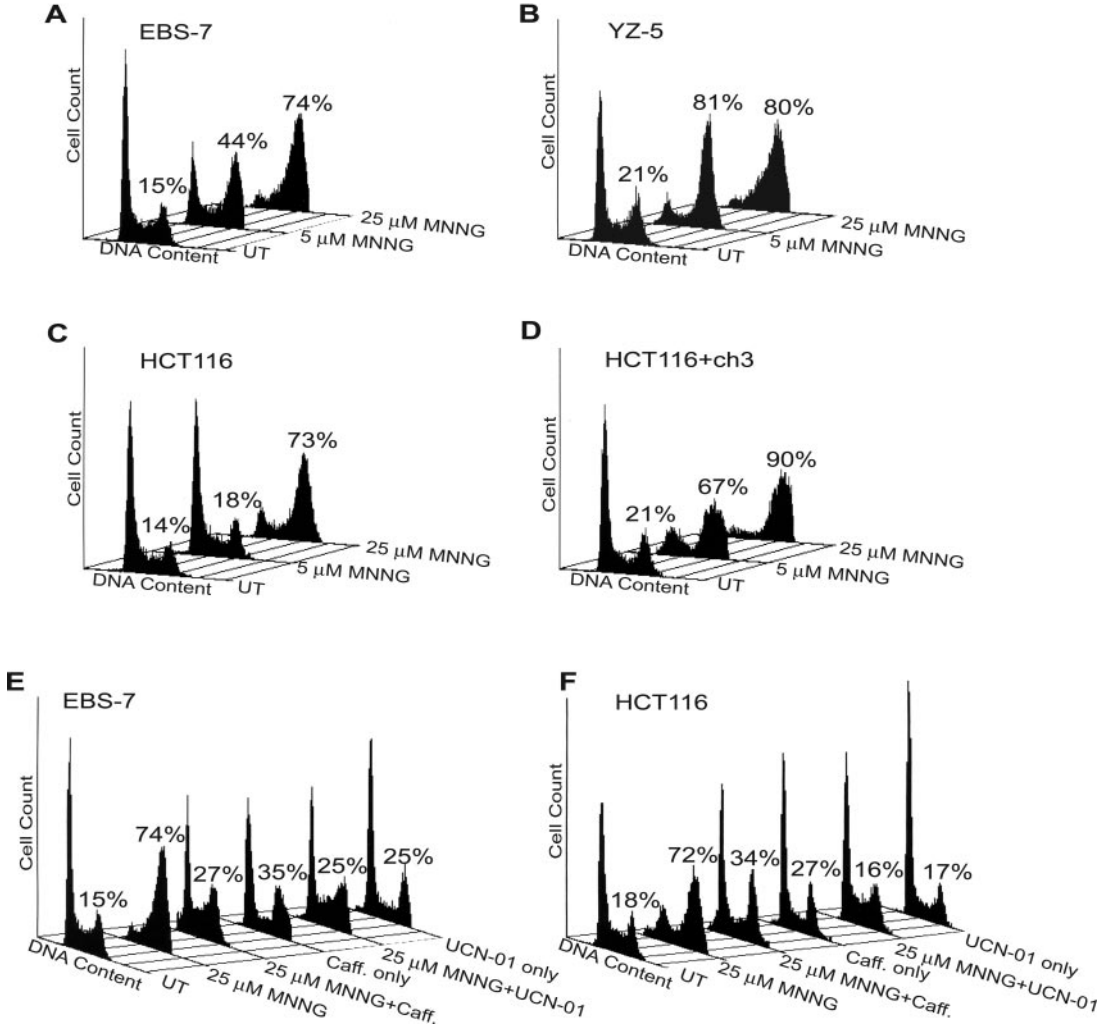

Fig. 1. High-dose MNNG exposure activates an ATM- and MMR-independent G_2 arrest that is abrogated by the pharmacological inhibitors caffeine and UCN-01. A, ATM-deficient EBS-7 fibroblasts were either mock-treated or exposed to 5 or 25 μM MNNG, harvested at 48 h, fixed, stained with propidium iodide, and analyzed by flow cytometry. The percentage of cells in the histogram containing 4N DNA content is indicated. B, ATM-proficient YZ-5 fibroblasts were treated and analyzed as outlined in A. C, MMR-deficient HCT116 colorectal tumor cells were treated and analyzed as outlined in A. D, MMR-proficient HCT116+ch3 cells were treated and analyzed as outlined in A. E, EBS-7 cells were pretreated with 5 mM caffeine for 1 h before exposure to 25 μM MNNG, and caffeine was maintained in the growth medium throughout the incubation period. Otherwise, EBS-7 cells were pretreated with 500 nM UCN-01 for 45 min before MNNG exposure, and UCN-01 was maintained in the growth medium throughout the incubation period. Mock-treated, 25 μM MNNG-only treated, 25 μM MNNG + caffeine-treated, caffeine only-treated, 25 μM MNNG + UCN-01–treated, and UCN-01 only-treated cells were harvested 48 h after MNNG treatment and then fixed, stained with propidium iodide, and analyzed by flow cytometry. The percentage of cells displaying a 4N DNA content is noted. F, HCT116 cells were treated and analyzed as outlined in E.

Chk2 occurs in an MMR-dependent manner, whereas Chk2 activation also requires ATM activity (Adamson et al., 2005). To determine whether Chk1 and/or Chk2 are activated during their response to high-dose MNNG exposure, we assessed the phosphorylation state of these molecules in EBS-7 and HCT116 cells after treatment with 25 μM MNNG. Immunoblot analysis of extracts formed from 25 μM MNNG-treated EBS-7 cells with phospho-Ser317 Chk1-specific antibody, a post-translational modification linked to catalytic activation of this kinase (Zhao and Piwnica-Worms, 2001), detected an increase in Chk1 phosphorylation with 5 μM MNNG treatment (Fig. 3A). This agrees with previous findings indicating that Chk1 activation occurs in an ATM-independent manner in response to MNNG. However, we measured a notable increase in Chk1 phosphorylation (1.9-fold) in extracts from EBS-7 cells treated with 25 μM compared with those exposed to 5 μM MNNG. In MMR-deficient HCT116 cells, we again observed no Chk1 activation in response to 5 μM MNNG (Fig. 3B). However, robust Chk1 Ser317 phosphorylation was evident in these cells in response to 25 μM MNNG. These experiments indicate that compared with the response mounted after exposure to a lower dose of MNNG, high-dose MNNG exposure results in heightened Chk1 activity in EBS-7 cells and promotes activation of Chk1 through an MMR-independent mechanism.

Extracts from MNNG-treated EBS-7 and HCT116 cells

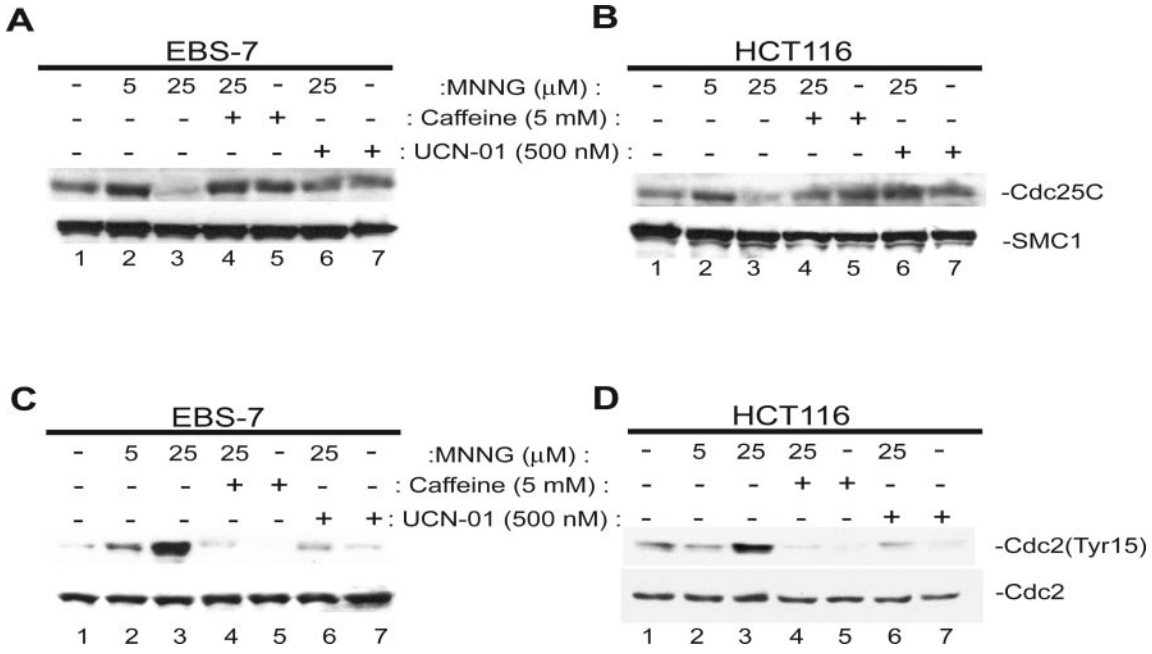

Fig. 2. Nuclear exclusion of Cdc25C and accumulation of inactive Cdc2 occur in an ATM- and MMR-independent manner after high-dose MNNG exposure. A, EBS-7 cells were either mock-treated (lane 1), 5 μM MNNG-treated (lane 2), 25 μM MNNG-treated (lane 3), pretreated for 1 h and maintained on 5 mM caffeine after 25 μM MNNG treatment (lane 4), caffeine-treated only (lane 5), pretreated for 45 min and maintained on UCN-01 after 25 μM MNNG treatment (lane 6), or UCN-01–treated only (lane 7). Cells were harvested 48 h after MNNG exposure and were subsequently fractionated into nuclear and cytoplasmic fractions. These nuclear fractions were immunoblotted with anti-Cdc25C (top) or SMC1 (bottom; nuclear fraction loading control). B, HCT116 cells were analyzed as outlined in A. C, EBS-7 cells were treated as outlined in A; however, total cell lysates were formed from the harvested cells, and these were subjected to immunoblot analysis with phospho-Tyr15 Cdc2-specific antibody (top) or anti-total Cdc2 (bottom) to confirm equal protein abundance. D, HCT116 cells were analyzed as outlined in C.

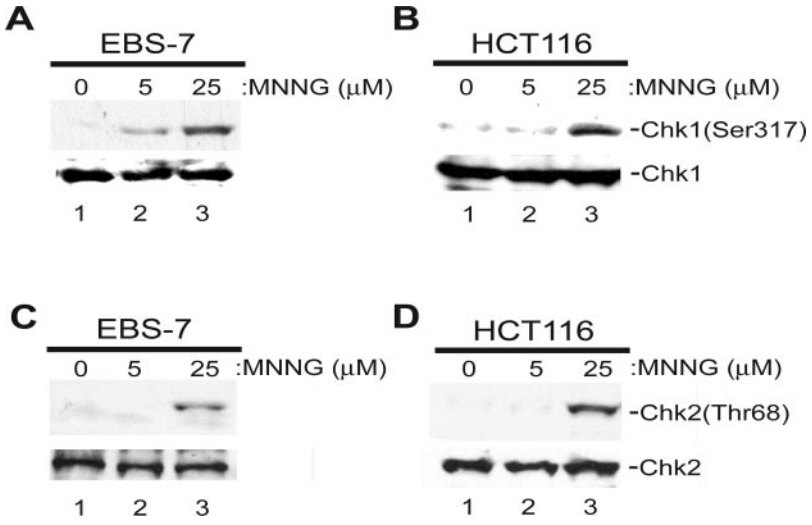

Fig. 3. Neither ATM nor MMR is required for activation/phosphorylation of Chk1 or Chk2 after high-dose exposure to MNNG. A, EBS-7 cells were either mock-treated (lane 1), treated with 5 μM MNNG (lane 2), or treated with 25 μM MNNG (lane 3). Cells were harvested 48 h after MNNG exposure, and the extracts were immunoblotted with phospho-Ser317 Chk1-specific antibody (top) or anti-total Chk1 (bottom). B, HCT116 were treated and analyzed as described in A. C, EBS-7 extracts were analyzed by immunoblotting with phospho-Thr68 Chk2-specific antibody (top) or anti-total Chk2 (bottom). D, HCT116 extracts were analyzed as outlined in C.

were also assayed for phosphorylation of the Thr68 residue of Chk2. Phosphorylation of this residue is linked to activation of the Chk2 kinase (Matsuoka et al., 2000). EBS-7 cells displayed no Chk2 phosphorylation in response to 5 μM MNNG, reinforcing the ATM-dependence of Chk2 phosphorylation in response to moderate doses of MNNG (Fig. 3C). However, prominent phosphorylation of Chk2 was detected in EBS-7 cells treated with 25 μM MNNG. As shown previously, HCT116 cells treated with 5 μM MNNG exhibited no detectable Chk2 phosphorylation (Fig. 3D). However, exposure to 25 μM MNNG resulted in significant Chk2 phosphorylation. These results indicate that unlike the MMR and ATM-dependent nature of Chk2 phosphorylation/activation observed in response to moderate doses of MNNG, activation of Chk2 in response to high-dose MNNG exposure is not dependent on either ATM or MMR.

ATR Is Required for Chk1 Activation and Establishment of G_2 Arrest in Response to High-Dose MNNG Exposure. In light of the inhibitory effect of caffeine on G_2 arrest and the ATM-independent nature of both checkpoint activation and Chk1 and Chk2 activation, we hypothesized that ATR activity is essential to triggering G_2 arrest in response to high-dose MNNG exposure. To address this question, we tested the $ATR^{flox/-}$ cell line (Cortez et al., 2001).

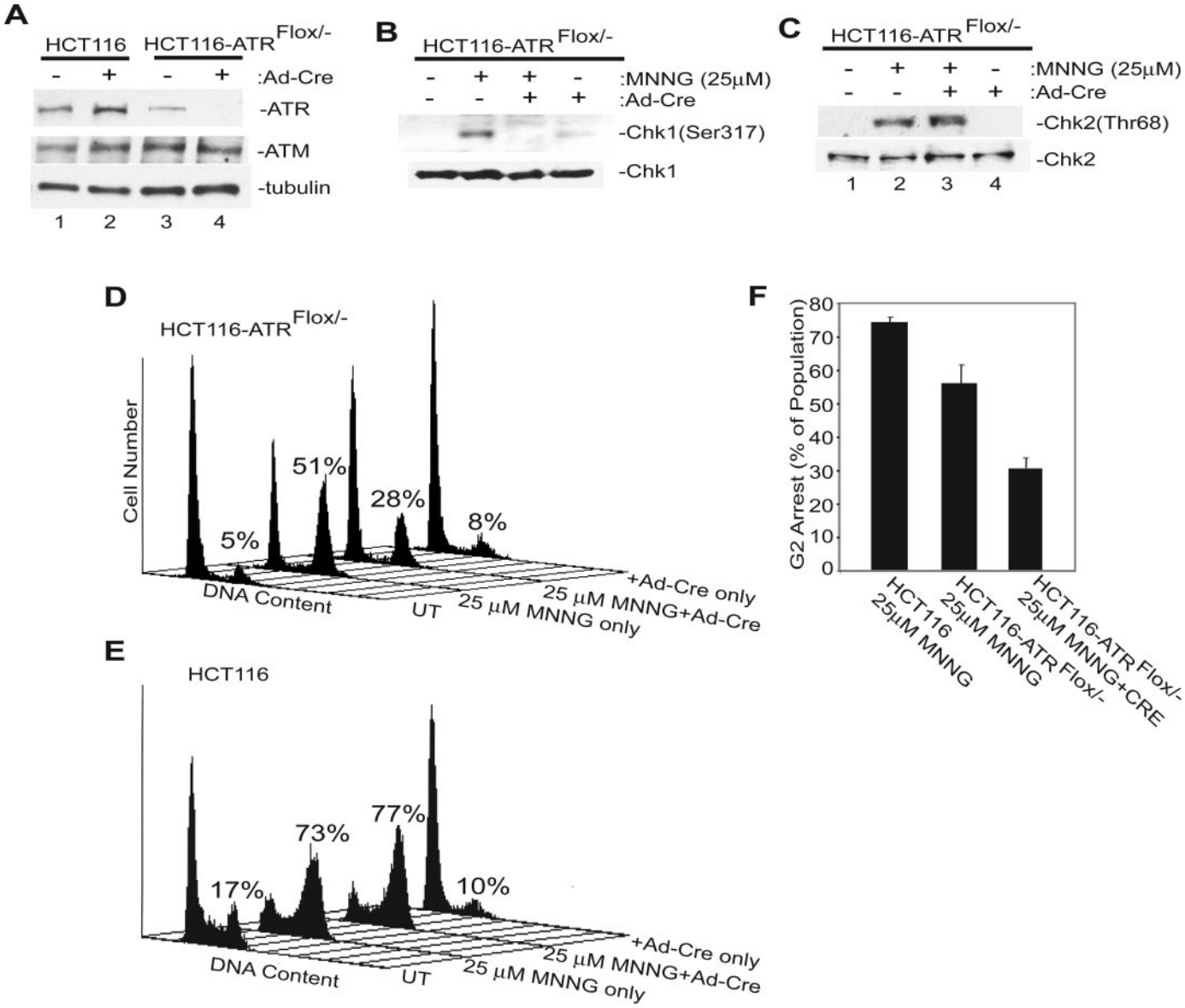

Fig. 4. ATR is required for Chk1 activation of and establishment of G_2 arrest after high-dose MNNG treatment. A, HCT116 (lanes 1 and 2) or $ATR^{flox/-}$ (lanes 3 and 4) were either mock-infected (lanes 1 and 3) or infected with adenovirus (lanes 2 and 4) expressing Ad-Cre. Forty-eight hours after viral infection, cells were harvested, and lysates were formed and subjected to immunoblot analysis with anti-ATR (top), anti-ATM (middle), or anti-tubulin (bottom) as a protein loading control. B, $ATR^{flox/-}$ cells were either mock-treated (lane 1), 25 μM MNNG-treated (lane 2), 25 μM MNNG-treated 48 h after Ad-Cre infection (lane 3), or infected with Ad-Cre only (lane 4). Forty-eight hours after MNNG exposure, cells were harvested, and extracts were formed and subsequently immunoblotted with phospho-Ser317 Chk1-specific antibody (top) or anti-total Chk1 (bottom). C, extracts outlined in B were immunoblotted with phospho-Thr68 Chk2-specific antibody (top) or anti-total Chk2 (bottom). D, $ATR^{flox/-}$ cells were either mock-treated, 25 μM MNNG-treated, 25 μM MNNG-treated 48 h after Ad-Cre infection, or were only Ad-Cre–infected. Cells were harvested 48 h after MNNG exposure, fixed, stained with propidium iodide, and subsequently analyzed by flow cytometry. The percentage of cells containing 4N DNA is indicated. E, HCT116 cells were treated and analyzed as outlined in D. F, the mean percentages of G_2-arrested cells measured in three independent experiments conducted on 25 μM MNNG-treated HCT116, uninfected $ATR^{flox/-}$, and Ad-Cre–infected $ATR^{flox/-}$ cells are plotted. Error bars, 1.0 S.D.

This cell line is a derivative of HCT116 that contains one disrupted ATR allele, and the other ATR allele has been engineered to contain loxP sites flanking exon 2. Expression of Cre recombinase results in the efficient excision of exon 2, resulting in the introduction of a frameshift mutation within the ATR transcript and consequential premature truncation of the ATR protein. Therefore, Cre recombinase expression results in the conditional loss of ATR expression. Treatment of the parental HCT116 line with Ad-Cre for 48 h resulted in no detectable decrease in ATR expression (Fig. 4A, top). As shown previously (Cortez et al., 2001), ATR abundance in uninfected $ATR^{flox/-}$ cells was diminished compared with the parental HCT116 line containing two functional ATR alleles, and Ad-Cre infection of $ATR^{flox/-}$ cells resulted in a dramatic decrease in ATR abundance. To ensure that ATM expression was unaltered in these cells, these extracts were also immunoblotted with anti-ATM (Fig. 4A, middle). Both HCT116 and $ATR^{flox/-}$ lines displayed no detectable alterations in ATM expression, regardless of Ad-Cre infection.

Next, we immunoblotted extracts of MNNG-treated $ATR^{flox/-}$ cells with phosphospecific Chk1 and Chk2 antibodies. We observed the activation of Chk1 after 25 μM MNNG treatment in $ATR^{flox/-}$ cells not infected with Ad-Cre (Fig. 4B). After Ad-Cre infection, however, $ATR^{flox/-}$ cells displayed no detectible Chk1 activation in response to 25 μM MNNG. Furthermore, Ad-Cre infection alone had no detectable effect on the accumulation of phosphorylated Chk1. These lysates were also assessed for Chk2 phosphorylation/activation. Again, we observed significant Chk2 phosphorylation in response to 25 μM MNNG in uninfected $ATR^{flox/-}$ cells (Fig. 4C). Furthermore, no Chk2 phosphorylation was observed in response to Ad-Cre infection alone. In direct contrast to Chk1 phosphorylation, robust phosphorylation of Chk2 was observed after 25 μM MNNG in Ad-Cre infected in $ATR^{flox/-}$ cells. These results argue against a strict requirement for ATR in the activation of Chk2 in response to 25 μM MNNG, and because ATM is present in these cells (Fig. 4A), it is likely that Chk2 is activated by ATM in ATR-deficient cells.

Flow cytometry was subsequently performed in uninfected and Ad-Cre–infected $ATR^{flox/-}$ cells and HCT116 cells treated in parallel. We observed typical robust G_2 arrest (73%) 48 h after 25 μM MNNG treatment in the parental HCT116 cell line (Fig. 4D). Furthermore, MNNG-induced G_2 arrest in HCT116 was unaltered by infection with Ad-Cre. In uninfected $ATR^{flox/-}$ cells, exposure to 25 μM MNNG resulted in less robust accumulation of cells arrested in G_2 (51%) compared with the response observed uninfected HCT116. This outcome is probably the result of decreased expression of ATR in the $ATR^{flox/-}$ cells compared with the parental line. Consistent with this interpretation, a reduction in G_2 arrest (28%) was observed in MNNG-treated, Ad-Cre–infected $ATR^{flox/-}$ cells. In both HCT116 and $ATR^{flox/-}$ lines, we found that Ad-Cre infection alone did not induce G_2 arrest. Analysis of three independent experiments (Fig. 4F) indicate that 25 μM MNNG-treated $ATR^{flox/-}$ cells display a statistically significant decrease in G_2 arrest ($p = 0.005$, Student's t test, two-sided) compared with MNNG-treated HCT116 cells, and Ad-Cre infection of $ATR^{flox/-}$ cells resulted in a highly significant decrease in MNNG-induced G_2 arrest ($p = 2.5 \times 10^{-5}$) compared with HCT116. The interpretation that this diminished G_2 arrest is attributable to reduced ATR expression is supported by the observation that MNNG-treated, Ad-Cre infected $ATR^{flox/-}$ cells display a significant ($p = 0.002$) reduction in G_2 arrest compared with uninfected MNNG-treated $ATR^{flox/-}$ cells. Because measurable G_2 arrest was observed in MNNG-treated, Ad-Cre–infected $ATR^{flox/-}$ cells, we cannot strictly conclude that ATR is sufficient to induce G_2 arrest in response to high-dose MNNG exposure. However, from these findings, we do conclude that ATR is required for activation of Chk1 but not Chk2, and that ATR, but not ATM, is required for establishing G_2 arrest in response to high-dose MNNG exposure.

High-Dose MNNG-Induced G_2 Arrest Is Chk2-Independent. The findings outlined above indicate that the cell-cycle arrest triggered by high-dose MNNG exposure is ATR-dependent and that this correlates with ATR-dependent Chk1 activation. However, Chk2 was robustly phosphorylated/activated in response to 25 μM MNNG. To test a potential role for Chk2 in the activation of G_2 arrest in response to high-dose MNNG exposure, we obtained an HCT116 derivative cell line deficient in Chk2 (Jallepalli et al., 2003). Immunoblot analysis of these cells confirmed Chk2 deficiency and indicated that Chk1 abundance was unaltered in HCT116 $Chk2^{-/-}$ cells (Fig. 5A). In response to 25 μM MNNG exposure, HCT116 $Chk2^{-/-}$ cells exhibited a robust (66%) G_2 arrest 48 h after drug exposure. In addition, pretreatment and maintenance of these cells on UCN-01 during and after 25 μM MNNG treatment completely abrogated G_2 arrest in this cell line (Fig. 5B). As a result of this finding, we conclude that the ATM/Chk2 pathway is not required for G_2 checkpoint signaling in response to high doses of MNNG.

Chk1 Is Required for Establishment of G_2 Arrest after High-Dose MNNG Exposure. The results outlined

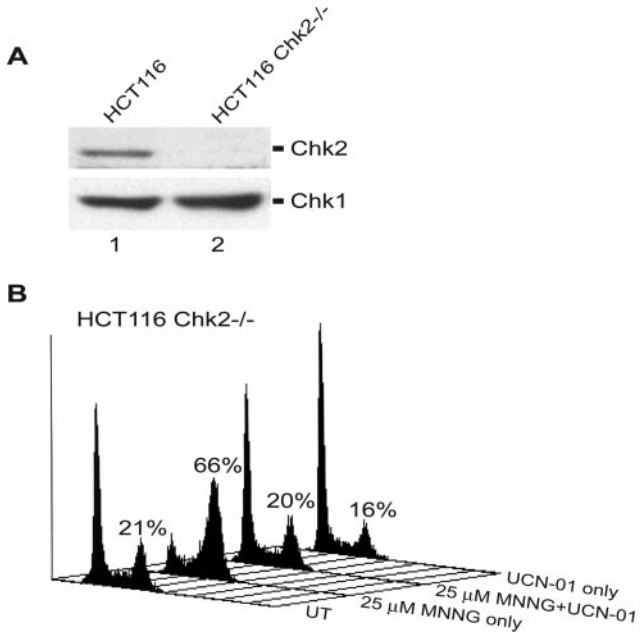

Fig. 5. Chk2 is not required for the activation of G_2 arrest in response to high-dose MNNG exposure. A, extracts of HCT116 (lane 1) and HCT116 $Chk2^{-/-}$ (lane 2) cells were immunoblotted with anti-Chk2 (top) or anti-Chk1 (bottom) antibody. B, HCT116 $Chk2^{-/-}$ cells were either mock-treated, 25 μM MNNG-treated, pretreated for 45 min and maintained on 500 nM UCN-01 during and after 25 μM MNNG treatment, or treated with 500 nM UCN-01 only. Forty-eight hours after MNNG exposure, cells were harvested, fixed, stained with propidium iodide, and analyzed by flow cytometry. The percentage of cells with 4N DNA content is indicated.

above indicate the importance of ATR in activation of the G_2 checkpoint in response to high-dose MNNG exposure. To ascertain that the ATR/Chk1 pathway is involved in triggering high-dose MNNG-induced G_2 arrest, we used RNA interference (RNAi) technology to reduce Chk1 expression in cultured cells. First, we used HCT116 $Chk2^{-/-}$ cells to uniquely isolate the role of Chk1 in activating this checkpoint. Immunoblot analysis of HCT116 $Chk2^{-/-}$ cells transfected with pooled, Chk1-specific siRNA duplexes documented a 2.5-fold reduction of total Chk1 compared with mock-transfected (no siRNA) or control-transfected (nontarget siRNA) cells (Fig. 6A). When these cells were treated with 25 μM MNNG and assayed by flow cytometry 48 h after drug, we observed that mock- and control-transfected cells displayed a robust G_2 blockade (63%) (Fig. 6B). Cells transfected with Chk1-specific siRNA and subsequently treated with 25 μM MNNG displayed a reduced percentage of cells in G_2 (52%). This ~16% reduction in G_2-arrested cells supports the notion that Chk1 is a necessary molecular component in the G_2 checkpoint pathway activated in response to high-dose MNNG.

Although consistently reproducible, the reduction in G_2 arrest produced by siRNA-mediated Chk1 depletion was notably modest compared with results obtained in Chk1 siRNA-transfected cells treated with 5 μM MNNG (Adamson et al., 2005). In a previous study, we observed a reproducible ~50% reduction in 5 μM MNNG-induced G_2 arrest in HCT116+ch3 cells transfected with Chk1 siRNA. We hypothesized that the more subtle effects observed in cells treated with 25 μM are attributable to increased Chk1 catalytic activity in cells treated with 25 μM compared with Chk1 activity in cells treated with 5 μM MNNG. This thinking stemmed from our observation that the accumulation of phosphorylated/activated Chk1 in MNNG-treated EBS-7 cells is 1.9-fold higher in cells treated with 25 μM than in cells treated with 5 μM (Fig. 3A). To confirm that this dose-dependent increase in Chk1 phosphorylation/activation is a general phenomenon, we treated HCT116+ch3 cells with 5 and 25 μM MNNG and subjected lysates from these cells to immunoblot analysis with phospho-Ser317 Chk1-specific antibody. Similar to our previous findings using EBS-7 cells, we observed that HCT116+ch3 cells treated with 25 μM MNNG displayed a 2.2-fold elevated level of phosphorylated/activated Chk1 compared with cells treated with 5 μM MNNG (Fig. 6C). From these observations, we conclude that higher doses of MNNG trigger a more robust activation of Chk1.

Next, we conducted flow cytometry analysis on Chk1 siRNA-transfected HCT116+ch3 cells treated with either 5 or 25 μM MNNG. We observed, in close agreement with results obtained from similarly manipulated HCT116 $Chk2^{-/-}$ cells, that transfection with pooled, Chk1-specific siRNA resulted in a 4.9-fold reduction in Chk1 expression in HCT116+ch3 cells compared with compared with mock- and control siRNA-transfected cells (Fig. 6D). Furthermore, flow cytometry analysis of mock- and control siRNA-transfected HCT116+ch3 cells treated with either 5 or 25 μM MNNG indicated that these manipulations resulted in no apparent diminishment in G_2 arrest at either MNNG dose (Fig. 6E). Flow cytometry also revealed that Chk1-depleted HCT116+ch3 cells treated with 5 μM MNNG showed a 37% reduction in G_2 arrested cells compared with mock-transfected cells treated with this dose of MNNG. In contrast, and consistent with results from experiments on HCT116 $Chk2^{-/-}$ cells, Chk1 siRNA-transfected HCT116+ch3 cells treated with 25 μM MNNG displayed a 20% reduction in G_2-arrested cells compared with 25 μM MNNG treated, mock-transfected cells. Analysis of three independent experiments indicate that siRNA-mediated knockdown of Chk1 expression in HCT116+ch3 cells treated with 25 μM MNNG led to a statistically significant decrease in G_2 arrest ($p = 0.012$) compared with 25 μM MNNG-treated HCT116+ch3 cells transfected with control siRNA. Furthermore, 25 μM MNNG-treated HCT116+ch3 cells transfected with Chk1 siRNA showed a highly significant ($p = 7.8 \times 10^{-5}$) reduction in G_2 arrest compared with 25 μM MNNG-treated HCT116+ch3 cells transfected with control siRNA. It is noteworthy that a statistically significant ($p = 0.005$) difference between the percentage of G_2-arrested cells in populations of Chk1 siRNA-transfected HCT116+ch3 cells treated with 5 or 25 μM MNNG was observed. From these experiments, we conclude that siRNA-mediated knockdown of Chk1 produces a more significant effect on G_2 arrest in response to moderate doses of MNNG compared with response to high-dose MNNG exposure. Moreover, it is reasonable to speculate that this effect stems, in part, from heightened Chk1 activity in cells treated with higher doses of this alkylating agent.

Discussion

MNNG-Induced Checkpoint Signaling: High- Versus Moderate-Dose Response. It has long been established that G_2 checkpoint activation in response to S_N1-alkylating agents is triggered via an MMR-dependent mechanism (Goldmacher et al., 1986; Kat et al., 1993; Koi et al., 1994; Hawn et al., 1995). We and others (Jaiswal et al., 2004; Stojic et al., 2005), however, have observed that substantially higher doses of MNNG triggered G_2 arrest in MMR-deficient cells. Here, we document that in cells treated with high-dose MNNG, both Chk1 and Chk2 are activated in an MMR-independent fashion. The MNNG-induced G_2 checkpoint occurs independently of ATM, Chk2, and MMR, and checkpoint establishment is reliant on the ATR/Chk1 signaling pathway. Compared with earlier studies that examined mechanisms responsible for MMR-dependent G_2 arrest (Stojic et al., 2004b; Adamson et al., 2005), we conclude that MNNG activates the G_2 checkpoint through various pathways, and these different mechanisms are activated in a dose-dependent manner.

We observed that caffeine and UCN-01 blocked the establishment of the G_2 checkpoint in response to high-dose MNNG exposure. These drugs exerted similar effects in response to moderate doses of MNNG (Adamson et al., 2005). We also examined the effects of these agents on two downstream events linked to G_2 checkpoint establishment: Cdc25C and Cdc2 inactivation. Our previous work demonstrated that inactivation of these molecules in response to moderate doses of MNNG was dependent on a functional MMR system, indicating that Cdc25C and Cdc2 are targeted for inactivation in response to MNNG (Adamson et al., 2005). Our present findings indicate that Cdc25C and Cdc2 are also inactivated in response to high-dose MNNG exposure; thus, both moderate-dose and high-dose response use, at least in part, similar downstream mechanisms to block cell-cycle advance. However, it bears consideration that other G_2 check-

point pathways may be activated in response to MNNG and other genotoxic drugs. Additional investigation is clearly required to fully elucidate the mechanisms that halt cell-cycle advance at the G_2/M transition point.

One of the prominent dissimilarities between response to moderate doses of MNNG (MMR-dependent G_2 arrest-activated) and high doses of MNNG (MMR-independent G_2 arrest-activated) is differences in Chk1 and Chk2 activation. In response to IR, Chk2 is activated by ATM through phosphorylation of the Thr68 residue (Matsuoka et al., 2000). Mat-

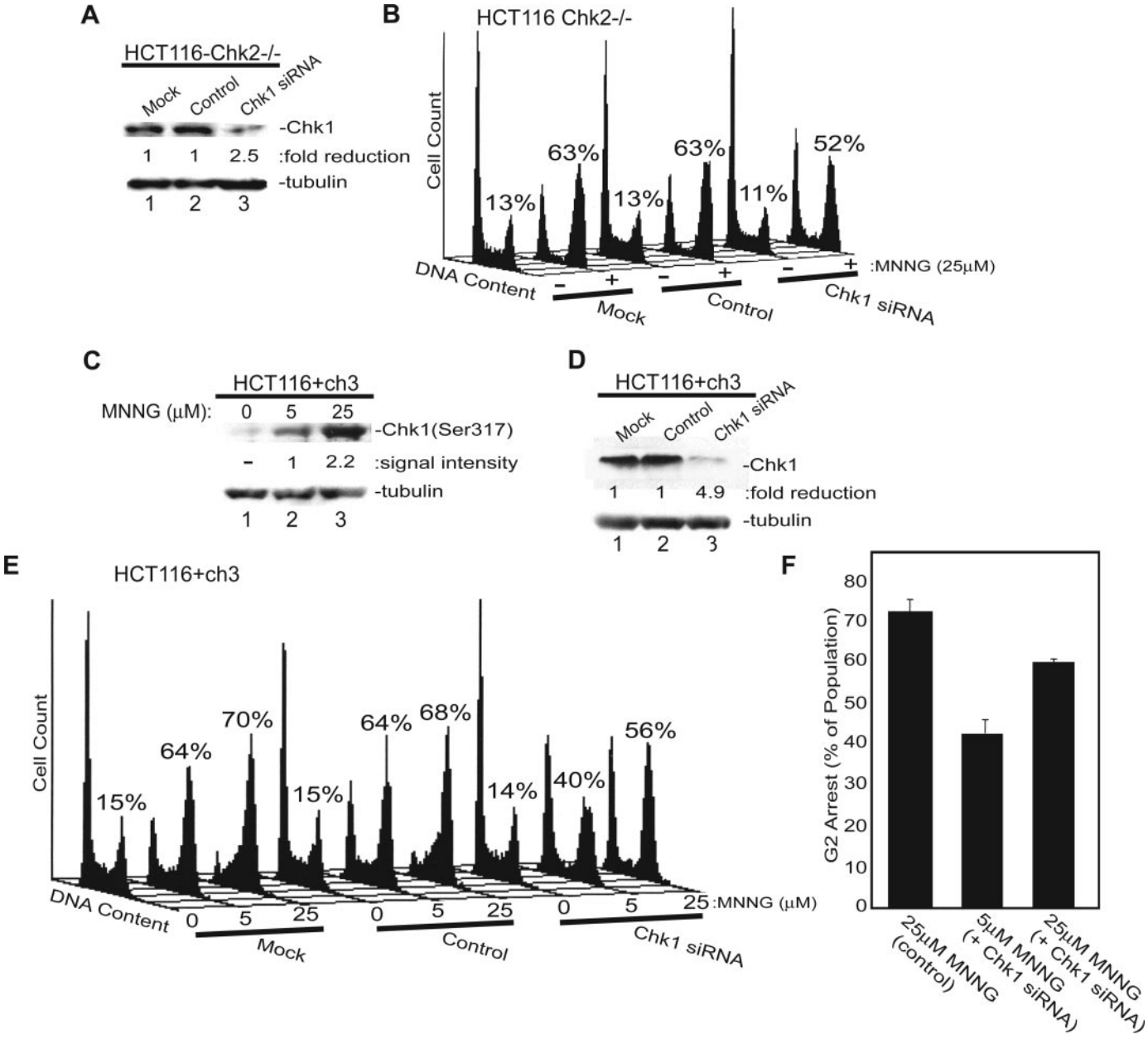

Fig. 6. RNAi-induced depletion of Chk1 results in diminished establishment of G_2 arrest after high-dose MNNG exposure. A, HCT116 Chk2$^{-/-}$ cells were either mock-transfected (lane 1), transfected with nontarget control siRNA (lane 2), or transfected with pooled Chk1-specific siRNA (lane 3). Forty-eight hours after transfection, cells were immunoblotted with anti-total Chk1 (top) or anti-tubulin (bottom) to confirm equivalent loading. The fold reduction in Chk1 expression is indicated as measured by analysis of exposed autoradiography films. B, HCT116 Chk2$^{-/-}$ cells were either mock-transfected, transfected with nontarget siRNA, or transfected with Chk1-specific siRNA. After this, cultures were evenly divided, and cells were mock-treated or exposed to 25 μM MNNG, harvested 48 h later, and analyzed by flow cytometry. The percentage of cells containing 4N DNA content is indicated. C, HCT116+ch3 cells were either mock-treated (lane 1), 5 μM MNNG-treated (lane 2), or 25 μM MNNG-treated (lane 3). Cells were harvested 48 h after drug treatment, lysed, and immunoblotted with phospho-Ser317 Chk1-specific antibody (top) and anti-total Chk1 (bottom). The relative intensity of the phosphorylated Chk1 signal is indicated. D, HCT116+ch3 cells were either mock-transfected (lane 1), transfected with nontarget control siRNA (lane 2), or transfected with pooled Chk1-specific siRNA (lane 3), and 48 h after transfection, the cell extracts were immunoblotted with anti-total Chk1 (top) and anti-tubulin (bottom). E, HCT116+ch3 cells were either mock-transfected, transfected with nontarget control siRNA, or transfected with Chk1-specific siRNA. After this, cultures were divided into three equal pools. These pools were either mock-treated, treated with 5 or 25 μM MNNG, harvested 48 h later, and analyzed by flow cytometry. The percentage of cells displaying a 4N DNA content is indicated. F, the mean percentages of G_2-arrested cells measured in three independent experiments conducted on 25 μM MNNG-treated HCT116+ch3 transfected with either control siRNA or Chk1 siRNA, or HCT116+ch3 cells transfected with Chk1 siRNA and treated with 5 μM MNNG are plotted. Error bars, 1.0 S.D.

suoka et al. (1998) also determined that Chk2 was activated in an ATM-independent manner in response to hydroxyurea and UV light and that this was most likely attributable to ATR activity. Here, we document that Chk2 activation is ATM-independent during high-dose MNNG response, and because ATR is activated in response to MNNG, it is plausible that ATR is responsible for the Chk2 phosphorylation observed in ATM-deficient cells after high-dose MNNG exposure. ATM-independent Chk2 activation also occurs in response to high-dose IR exposure (Matsuoka et al., 1998), suggesting that dose-responsive activation of Chk2 by ATR may be a general phenomenon after genotoxin exposure. It also bears consideration that the ATM and ATR-related kinase DNA-PK has recently been shown to phosphorylate Chk2 as well (Li and Stern, 2005).

In response to replication block and UV light, ATR activates Chk1 (Liu et al., 2000). Although Chk1 phosphorylation in response to IR seems somewhat reduced compared with UV-induced response (Zhou and Elledge, 2000), Chk1 is required for the activation of G_2 arrest in response to IR (Liu et al., 2000). MMR-deficient cells fail to activate Chk1 in response to MNNG doses, resulting in MMR-dependent G_2 arrest (Stojic et al., 2004b; Adamson et al., 2005). Herein, we show that high-dose MNNG exposure results in the phosphorylation of Chk1 via an MMR-independent mechanism, and Chk1 is required to establish G_2 arrest in response to high-dose MNNG exposure. Taken together, these findings indicate that although Chk1 is activated through differing mechanisms, depending on the extent of MNNG-induced lesions, Chk1 is an indispensable component in the G_2 checkpoint machinery.

In contrast to our previous study in which we observed that RNAi-induced depletion of Chk2 resulted in diminished G_2 checkpoint activation after moderate doses of MNNG (Adamson et al., 2005), we document that Chk2-deficient cells show no observable perturbation in G_2 arrest after high doses of MNNG, but Chk1 is required for establishment of this checkpoint. Despite their structural dissimilarity, common downstream targets for Chk1 and Chk2, such as p53, Cdc25A, and Cdc25C, exist (Sanchez et al., 1997; Matsuoka et al., 1998; Chehab et al., 2000; Shieh et al., 2000; Falck et al., 2001; Zhao et al., 2002). By using peptide libraries to assess Chk1 and Chk2 substrate specificity, O'Neill et al. (2002) found substantial differences between these two serine/threonine kinases. This finding supports the view that Chk1 and Chk2 are only partially redundant in function and that there are probably distinct damage-responsive Chk1- or Chk2-dependent pathways. We documented that 25 μM MNNG results in a quantitatively higher level of phosphorylated Chk1 compared with response to 5 μM MNNG in two distinct cell lines (e.g., EBS-7 and HCT116+ch3). It is therefore possible that in response to high-dose MNNG exposure, Chk1-dependent checkpoint pathways are activated that are either inactive or minimally active during response to lower doses of MNNG. In this scenario, Chk2 activity would be required to fully activate the G_2 checkpoint in response to moderate doses of MNNG by promoting full activation of redundant pathways or activating other Chk2-dependent mechanisms. On the other hand, heightened Chk1 activity produced during response to a high dose may override the Chk2 requirement observed at lower doses of MNNG. This effect is possible by either potently activating redundant pathways or triggering other nonredundant mechanisms not activated in response to moderate-dose exposure. A more comprehensive understanding of pathways that establish the G_2 checkpoint is clearly needed to more precisely interpret the functional contribution of Chk1 and Chk2 to the triggering of this checkpoint.

Molecular Basis of Response to MNNG. MNNG exposure results in the methylation of multiple nucleophilic centers within the DNA molecule. *N*-Methylated purines (N^3A, N^7G) are recognized by specific DNA glycosylases and are repaired by BER, whereas O^6MeG is repaired by both direct repair and excision repair mechanisms. The DNA repair protein MGMT is responsible for the direct repair of O^6MeG by directly demethylation. In addition, the MMR system recognizes O^6MeG in either O6Me:T or O6Me:C base pairs (Griffin et al., 1994; Duckett et al., 1996). Persistent O^6MeG lesions are widely viewed as the lesions that trigger MMR-dependent checkpoint signaling (Bellacosa, 2001; Stojic et al., 2004a).

In response to high-dose MNNG exposure, however, there is no apparent requirement for MMR to trigger effective checkpoint signaling. This suggests that lesions other than O^6MeG activate checkpoint mechanisms. Methyl-methane sulfonate (MMS) is an S_N2-alkylating agent that primarily alkylates the N^3 position of adenine and N^7 position of guanine but alkylates the O^6 positions of guanine to a very small extent. Resultant MMS-generated N^3A and N^7G adducts are primarily repaired by BER. During BER, glycosylases hydrolyze the glycosidic bond between the nitrogenous base and the deoxyribose moiety in the DNA backbone, thus creating an apurinic/apyrimidinic (AP) site. Furthermore, because base alkylation weakens the glycosidic bond (Loeb and Preston, 1986), AP sites can arise without glycosylase activity. AP sites are subsequently recognized by an endonuclease that catalyzes AP site-directed strand scission (Demple et al., 1991). In vitro studies indicate that ligation of the newly synthesized DNA strand is the rate-limiting step in BER (Srivastava et al., 1998; Sung and Mosbaugh, 2003), explaining the occurrence of strand breaks in cells exposed to both S_N1 and S_N2 alkylators (Schwartz, 1989).

We have shown previously that 25 μM MNNG induces rapid catalytic activation of ATM and accumulation of DNA strand breaks, as scored by the Comet assay (Adamson et al., 2002). Stojic et al. (2005) showed recently that formation of γH2AX foci and activation of Chk1/2 also occur rapidly after high-dose MNNG exposure. Whereas both ATM activation and γH2AX are correlated with the presence of double-strand breaks (DSBs) in the genome (Abraham, 2001; Pilch et al., 2003), these biochemical events indicate that DSBs occur in response to high-dose MNNG exposure. DSBs generated by alkylators are caused by the simultaneous processing of clustered AP sites on opposite DNA strands (Lomax et al., 2004), and their abundance would be expected to be proportional to initial lesion load. However, given the ATM-independent nature of high-dose MNNG G_2 checkpoint activation, it is unlikely that MNNG-induced DSBs are the dominant lesion that triggers activation of this checkpoint.

Because of persistent *N*-alkylated bases and AP sites, MMS exposure results in the stalling of DNA replication (Tercero and Diffley, 2001). Electron microscopy has revealed that replication fork stalling results in the generation of long regions of single-stranded DNA (ssDNA) attributed to asymmetric DNA synthesis during replication of the damaged

template (Sogo et al., 2002). The ATR/ATRIP complex binds to the ssDNA binding protein RPA and that this association promotes localization of ATR to sites of stalled replication (Zou and Elledge, 2003). Although the importance of the recruitment of ATR to ssDNA remains in question (Ball et al., 2005), it is clear that ATR responds to stalled replication by activating Chk1 and a consequential checkpoint response (Sanchez et al., 1997; Liu et al., 2000; Zhao and Piwnica-Worms, 2001). Thus, it is formally possible that stalled replication is the dominant lesion to which the cells trigger a checkpoint response after high-dose MNNG exposure.

Acknowledgments

We thank Drs. A.W. Adamson and R. Baskaran for helpful insights and comments during performance of this study. We also thank Dr. Ray Braquet and Megan Bronson for technical assistance.

References

Abraham RT (2001) Cell cycle checkpoint signaling through the ATM and ATR kinases. *Genes Dev* **15:**2177–2196.

Adamson AW, Beardsley DI, Kim WJ, Gao Y, Baskaran R, and Brown KD (2005) Methylator-induced, mismatch repair-dependent G_2 arrest is activated through Chk1 and Chk2. *Mol Biol Cell* **16:**1513–1526.

Adamson AW, Kim WJ, Shangary S, Baskaran R, and Brown KD (2002) ATM is activated in response to MNNG-induced DNA alkylation. *J Biol Chem* **277:**38222–38229.

Ahn JY, Schwarz JK, Piwnica-Worms H, and Canman CE (2000) Threonine 68 phosphorylation by ataxia telangiectasia mutated is required for efficient activation of Chk2 in response to ionizing radiation. *Cancer Res* **60:**5934–5936.

Allen DM, van Praag H, Ray J, Weaver Z, Winrow CJ, Carter TA, Braquet R, Harrington E, Ried T, Brown KD, et al. (2001) Ataxia telangiectasia mutated is essential during adult neurogenesis. *Genes Dev* **15:**554–566.

Ball HL, Myers JS, and Cortez D (2005) ATRIP binding to RPA-ssDNA promotes ATR-ATRIP localization but is dispensable for Chk1 phosphorylation. *Mol Biol Cell* **16:**2372–2381.

Bellacosa A (2001) Functional interactions and signaling properties of mammalian DNA mismatch repair proteins. *Cell Death Differ* **8:**1076–1092.

Branch P, Aquilina G, Bignami M, and Karran P (1993) Defective mismatch binding and a mutator phenotype in cells tolerant to DNA damage. *Nature (Lond)* **362:**652–654.

Castedo M, Perfettini JL, Roumier T, Yakushijin K, Horne D, Medema R, and Kroemer G (2004) The cell cycle checkpoint kinase Chk2 is a negative regulator of mitotic catastrophe. *Oncogene* **23:**4353–4361.

Chehab NH, Malikzay A, Appel M, and Halazonetis TD (2000) Chk2/hCds1 functions as a DNA damage checkpoint in G_1 by stabilizing p53. *Genes Dev* **14:**278–288.

Cortez D, Guntuku S, Qin J, and Elledge SJ (2001) ATR and ATRIP: partners in checkpoint signaling. *Science (Wash DC)* **294:**1713–1716.

Demple B, Herman T, and Chen DS (1991) Cloning and expression of APE, the cDNA encoding the major human apurinic endonuclease: definition of a family of DNA repair enzymes. *Proc Natl Acad Sci USA* **88:**11450–11454.

Duckett DR, Drummond JT, Murchie AI, Reardon JT, Sancar A, Lilley DM, and Modrich P (1996) Human MutSα recognizes damaged DNA base pairs containing O6-methylguanine, O4-methylthymine, or the cisplatin-d(GpG) adduct. *Proc Natl Acad Sci USA* **93:**6443–6447.

Falck J, Mailand N, Syljuasen RG, Bartek J, and Lukas J (2001) The ATM-Chk2-Cdc25A checkpoint pathway guards against radioresistant DNA synthesis. *Nature (Lond)* **410:**842–847.

Goldmacher VS, Cuzick RA Jr, and Thilly WG (1986) Isolation and partial characterization of human cell mutants differing in sensitivity to killing and mutation by methylnitrosourea and N- methyl-N′-nitro-N-nitrosoguanidine. *J Biol Chem* **261:**12462–12471.

Graves PR, Yu L, Schwarz JK, Gales J, Sausville EA, O'Connor PM, and Piwnica-Worms H (2000) The Chk1 protein kinase and the Cdc25C regulatory pathways are targets of the anticancer agent UCN-01. *J Biol Chem* **275:**5600–5605.

Griffin S, Branch P, Xu YZ, and Karran P (1994) DNA mismatch binding and incision at modified guanine bases by extracts of mammalian cells: implications for tolerance to DNA methylation damage. *Biochemistry* **33:**4787–4793.

Hawn MT, Umar A, Carethers JM, Marra G, Kunkel TA, Boland CR, and Koi M (1995) Evidence for a connection between the mismatch repair system and the G2 cell cycle checkpoint. *Cancer Res* **55:**3721–3725.

Jaiswal AS, Multani AS, Pathak S, and Narayan S (2004) N-methyl-N′-nitro-N-nitrosoguanidine-induced senescence-like growth arrest in colon cancer cells is associated with loss of adenomatous polyposis coli protein, microtubule organization and telomeric DNA. *Mol Cancer* **3:**3.

Jallepalli PV, Lengauer C, Vogelstein B, and Bunz F (2003) The Chk2 tumor suppressor is not required for p53 responses in human cancer cells. *J Biol Chem* **278:**20475–20479.

Kalamegham R, Warmels-Rodenhiser S, MacDonald H, and Ebisuzaki K (1988) O^6-methylguanine-DNA methyltransferase-defective human cell mutant: O^6-methylguanine, DNA strand breaks and cytotoxicity. *Carcinogenesis* **9:**1749–1753.

Karran P and Bignami M (1992) Self-destruction and tolerance in resistance of mammalian cells to alkylation damage. *Nucleic Acids Res* **20:**2933–2940.

Kat A, Thilly WG, Fang WH, Longley MJ, Li GM, and Modrich P (1993) An alkylation-tolerant, mutator human cell line is deficient in strand-specific mismatch repair. *Proc Natl Acad Sci USA* **90:**6424–6428.

Kharbanda S, Saleem A, Datta R, Yuan ZM, Weichselbaum R, and Kufe D (1994) Ionizing radiation induces rapid tyrosine phosphorylation of p34cdc2. *Cancer Res* **54:**1412–1414.

Koi M, Umar A, Chauhan DP, Cherian SP, Carethers JM, Kunkel TA, and Boland CR (1994) Human chromosome 3 corrects mismatch repair deficiency and microsatellite instability and reduces *N*-methyl-*N*′-nitro-*N*-nitrosoguanidine tolerance in colon tumor cells with homozygous hMLH1 mutation. *Cancer Res* **54:**4308–4312.

Lee MS, Ogg S, Xu M, Parker LL, Donoghue DJ, Maller JL, and Piwnica-Worms H (1992) cdc25+ encodes a protein phosphatase that dephosphorylates p34cdc2. *Mol Biol Cell* **3:**73–84.

Li J and Stern DF (2005) Regulation of CHK2 by DNA-dependent protein kinase. *J Biol Chem* **280:**12041–12050.

Liu Q, Guntuku S, Cui XS, Matsuoka S, Cortez D, Tamai K, Luo G, Carattini-Rivera S, DeMayo F, Bradley A, et al. (2000) Chk1 is an essential kinase that is regulated by Atr and required for the G(2)/M DNA damage checkpoint. *Genes Dev* **14:**1448–1459.

Loeb LA and Preston BD (1986) Mutagenesis by apurinic/apyrimidinic sites. *Annu Rev Genet* **20:**201–230.

Lomax ME, Cunniffe S, and O'Neill P (2004) Efficiency of repair of an abasic site within DNA clustered damage sites by mammalian cell nuclear extracts. *Biochemistry* **43:**11017–11026.

Lopez-Girona A, Furnari B, Mondesert O, and Russell P (1999) Nuclear localization of Cdc25 is regulated by DNA damage and a 14–3-3 protein. *Nature (Lond)* **397:**172–175.

Masrouha N, Yang L, Hijal S, Larochelle S, and Suter B (2003) The *Drosophila* chk2 gene loki is essential for embryonic DNA double-strand-break checkpoints induced in S phase or G2. *Genetics* **163:**973–982.

Matsuoka S, Huang M, and Elledge SJ (1998) Linkage of ATM to cell cycle regulation by the Chk2 protein kinase. *Science (Wash DC)* **282:**1893–1897.

Matsuoka S, Rotman G, Ogawa A, Shiloh Y, Tamai K, and Elledge SJ (2000) Ataxia telangiectasia-mutated phosphorylates Chk2 in vivo and in vitro. *Proc Natl Acad Sci USA* **97:**10389–10394.

Meikrantz W, Bergom MA, Memisoglu A, and Samson L (1998) O6-alkylguanine DNA lesions trigger apoptosis. *Carcinogenesis* **19:**369–372.

Modrich P and Lahue R (1996) Mismatch repair in replication fidelity, genetic recombination and cancer biology. *Annu Rev Biochem* **65:**101–133.

O'Neill T, Giarratani L, Chen P, Iyer L, Lee CH, Bobiak M, Kanai F, Zhou BB, Chung JH, and Rathbun GA (2002) Determination of substrate motifs for human Chk1 and hCds1/Chk2 by the oriented peptide library approach. *J Biol Chem* **277:**16102–16115.

Paules RS, Levedakou EN, Wilson SJ, Innes CL, Rhodes N, Tlsty TD, Galloway DA, Donehower LA, Tainsky MA, and Kauffmann WK (1995) Defective G2 checkpoint function in cells from individuals with familial cancer syndromes. *Cancer Res* **55:**1763–1773.

Peng CY, Graves PR, Thoma RS, Wu Z, Shaw AS, and Piwnica-Worms H (1997) Mitotic and G2 checkpoint control: regulation of 14–3-3 protein binding by phosphorylation of Cdc25C on serine-216. *Science (Wash DC)* **277:**1501–1505.

Pilch DR, Sedelnikova OA, Redon C, Celeste A, Nussenzweig A, and Bonner WM (2003) Characteristics of gamma-H2AX foci at DNA double-strand breaks sites. *Biochem Cell Biol* **81:**123–129.

Sanchez Y, Wong C, Thoma RS, Richman R, Wu Z, Piwnica-Worms H, and Elledge SJ (1997) Conservation of the Chk1 checkpoint pathway in mammals: linkage of DNA damage to Cdk regulation through Cdc25. *Science (Wash DC)* **277:**1497–1501.

Sarkaria JN, Busby EC, Tibbetts RS, Roos P, Taya Y, Karnitz LM, and Abraham RT (1999) Inhibition of ATM and ATR kinase activities by the radiosensitizing agent, caffeine. *Cancer Res* **59:**4375–4382.

Sarkaria JN, Tibbetts RS, Busby EC, Kennedy AP, Hill DE, and Abraham RT (1998) Inhibition of phosphoinositide 3-kinase related kinases by the radiosensitizing agent wortmannin. *Cancer Res* **58:**4375–4382.

Schwartz JL (1989) Monofunctional alkylating agent-induced S-phase-dependent DNA damage. *Mutat Res* **216:**111–118.

Shieh SY, Ahn J, Tamai K, Taya Y, and Prives C (2000) The human homologs of checkpoint kinases Chk1 and Cds1 (Chk2) phosphorylate p53 at multiple DNA damage-inducible sites. *Genes Dev* **14:**289–300.

Singh SV, Herman-Antosiewicz A, Singh AV, Lew KL, Srivastava SK, Kamath R, Brown KD, Zhang L, and Baskaran R (2004) Sulforaphane-induced G2/M phase cell cycle arrest involves checkpoint kinase 2-mediated phosphorylation of cell division cycle 25C. *J Biol Chem* **279:**25813–25822.

Sogo JM, Lopes M, and Foiani M (2002) Fork reversal and ssDNA accumulation at stalled replication forks owing to checkpoint defects. *Science (Wash DC)* **297:**599–602.

Srivastava DK, Berg BJ, Prasad R, Molina JT, Beard WA, Tomkinson AE, and Wilson SH (1998) Mammalian abasic site base excision repair. Identification of the reaction sequence and rate-determining steps. *J Biol Chem* **273:**21203–21209.

Stojic L, Brun R, and Jiricny J (2004a) Mismatch repair and DNA damage signalling. *DNA Repair (Amst)* **3:**1091–1101.

Stojic L, Cejka P, and Jiricny J (2005) High doses of S_N1 type methylating agents activate DNA damage signaling cascades that are largely independent of mismatch repair. *Cell Cycle* **4:**473–477.

Stojic L, Mojas N, Cejka P, Di Pietro M, Ferrari S, Marra G, and Jiricny J (2004b) Mismatch repair-dependent G2 checkpoint induced by low doses of SN1 type methylating agents requires the ATR kinase. *Genes Dev* **18:**1331–1344.

Strausfeld U, Labbe JC, Fesquet D, Cavadore JC, Picard A, Sadhu K, Russell P, and Doree M (1991) Dephosphorylation and activation of a p34cdc2/cyclin B complex in vitro by human CDC25 protein. *Nature (Lond)* **351:**242–245.

Sung JS and Mosbaugh DW (2003) Escherichia coli uracil- and ethenocytosine-initiated base excision DNA repair: rate-limiting step and patch size distribution. *Biochemistry* **42:**4613–4625.

Tercero JA and Diffley JF (2001) Regulation of DNA replication fork progression through damaged DNA by the Mec1/Rad53 checkpoint. *Nature (Lond)* **412:**553–557.

Umar A, Koi M, Risinger JI, Glaab WE, Tindall KR, Kolodner RD, Boland CR, Barrett JC, and Kunkel TA (1997) Correction of hypermutability, *N*-methyl-*N*′-nitro-*N*-nitrosoguanidine resistance and defective DNA mismatch repair by introducing chromosome 2 into human tumor cells with mutations in MSH2 and MSH6. *Cancer Res* **57:**3949–3955.

Wang Y and Qin J (2003) MSH2 and ATR form a signaling module and regulate two branches of the damage response to DNA methylation. *Proc Natl Acad Sci USA* **100:**15387–15392.

Wei JH, Chou YF, Ou YH, Yeh YH, Tyan SW, Sun TP, Shen CY, and Shieh SY (2005) TTK/hMps1 participates in the regulation of DNA damage checkpoint response by phosphorylating CHK2 on threonine 68. *J Biol Chem* **280:**7748–7757.

Xu B, Kim ST, Lim DS, and Kastan MB (2002) Two molecularly distinct G_2/M checkpoints are induced by ionizing irradiation. *Mol Cell Biol* **22:**1049–1059.

Yu Q, La Rose J, Zhang H, Takemura H, Kohn KW, and Pommier Y (2002) UCN-01 inhibits p53 up-regulation and abrogates gamma-radiation-induced G_2-M checkpoint independently of p53 by targeting both of the checkpoint kinases, Chk2 and Chk1. *Cancer Res* **62:**5743–5748.

Zhao H and Piwnica-Worms H (2001) ATR-mediated checkpoint pathways regulate phosphorylation and activation of human Chk1. *Mol Cell Biol* **21:**4129–4139.

Zhao H, Watkins JL, and Piwnica-Worms H (2002) Disruption of the checkpoint kinase 1/cell division cycle 25A pathway abrogates ionizing radiation-induced S and G2 checkpoints. *Proc Natl Acad Sci USA* **99:**14795–14800.

Zhou BB and Elledge SJ (2000) The DNA damage response: putting checkpoints in perspective. *Nature (Lond)* **408:**433–439.

Ziv Y, Bar-Shira A, Pecker I, Russell P, Jorgensen TJ, Tsarfati I, and Shiloh Y (1997) Recombinant ATM protein complements the cellular A-T phenotype. *Oncogene* **15:**159–167.

Zou L and Elledge SJ (2003) Sensing DNA damage through ATRIP recognition of RPA-ssDNA complexes. *Science (Wash DC)* **300:**1542–1548.

Address correspondence to: Dr. K. D. Brown, Department of Biochemistry and Molecular Biology, University of Florida College of Medicine, 1600 SW Archer Road, Box 100245, Gainesville, FL 32611. E-mail: kdbrown1@ufl.edu